

Experimental evidence of a strange nonchaotic attractor in a Nd:YVO₄ laser with saturable absorber

Juliana N. Bourdieu,^{1,*} Mónica B. Agüero,^{1,2} and Marcelo G. Kovalsky^{1,2}

¹*Laboratorio de Láseres Sólidos, Centro de Investigación en Láseres y Aplicaciones (CEILAP), Instituto de Investigaciones Científicas y Técnicas para la Defensa (CITEDEF), Villa Martelli, Buenos Aires, Argentina.*

²*Consejo Nacional de Investigaciones Científicas y Técnicas (CONICET), Argentina.*

(Dated: April 17, 2025)

The diode-pumped Nd: Vanadate laser is one of the most widely used lasers in the near-infrared range. Using passive Q-switching with a Cr:YAG saturable absorber (SA), it generates nanosecond pulses at tens of kilohertz. This laser is known to exhibit low-dimensional deterministic chaos. In this letter, we present experimental evidence of a strange nonchaotic attractor (SNA). SNAs exhibit complex dynamical behavior that is neither periodic nor chaotic, making them difficult to detect in real-world systems. They are typically observed in systems modeled by equations and arise through a route to chaos. By experimentally obtaining time series of two laser variables, we reconstruct the underlying attractor. For a certain position of the SA, we find that all Lyapunov exponents are negative and that the energy spectra exhibit a broad frequency range, indicating that the attractor is nonchaotic and lacks periodicity. Using Higuchi's method, we estimate the fractal dimension (d_f) and find that 13% of the nonchaotic time series exhibit a well-defined non-integer d_f , confirming the presence of an SNA. To the best of our knowledge, this is the first experimental observation of a strange nonchaotic attractor in a complex optical system.

Introduction.—The study of attractors in nonlinear dynamical systems has been a cornerstone of chaos theory and complex systems research. While chaotic attractors, characterized by exponential sensitivity to initial conditions and fractal geometry, have been extensively studied since their first description by Ruelle and Takens [1], another intriguing class of attractors has emerged: strange nonchaotic attractors (SNAs). They were originally introduced in the 1980s by Grebogi et. al [2]. These attractors exhibit an unique combination of traits, merging the geometric complexity of strange attractors with the non-chaotic nature of systems characterized by non-positive Lyapunov exponents. Since their discovery, SNAs have been identified in various systems. In particular, experimental observations of SNAs have been documented in a magnetoelastic ribbon system under quasiperiodic driving [3], in electronic circuits [4, 5], in a memristor-based oscillator [6], and in an electrochemical cell [7]. In complex optical systems, such as lasers, chaotic attractors have been extensively studied both theoretically [8] and experimentally [9], since Haken [10] showed in 1975 that a single-mode laser is isomorphic to the Lorenz equations. One of the most popular and simple methods for generating pulses in the nanosecond range, widely used in scientific fields, as well as in defense and industry [11], is the passively Q-switched Nd:Vanadate laser, whose dynamics are well known [12, 13]. However, strange nonchaotic attractors (SNA) had not been reported until now. In this letter, we present experimental evidence of SNA in a solid-state Nd:Vanadate laser with a Cr:YAG crystal as a saturable absorber. By employing experimental time series of two laser's output variables, pulse amplitude and time between consecutive pulses, we are able to reconstruct an equivalent attractor. A control parameter al-

lows transitioning between the different dynamic behaviors of the laser.

Setup and measurements.—Our Nd:VO₄ laser operates in a standard V-shaped cavity. In Fig. 1, a schematic of our laser is shown. The cavity consists of a high-reflectivity (HR) concave mirror placed at the folding point of the cavity with a radius of curvature of 10 cm, and a plane output coupler with 99% reflectivity. The operating wavelength of the laser is 1064 nm and is linearly polarized. A solid-state saturable absorber (SA), Cr:YAG, with 90% unbleached transmission, is placed in the second arm of the cavity, between the folding mirror and the output coupler. The active medium is a $3 \times 3 \times 1$ mm Nd:VO₄ crystal, doped with 1%, and longitudinally pumped by a 2 W laser diode emitting at 808 nm.

The control parameter is the energy density over the SA, which is adjusted by varying the SA position within the laser cavity. Typical output of this laser is a pulse train with a repetition rate in the tens of kilohertz range and pulse duration of approximately 150 ns. The dynamic regimen of the laser output strongly depends on the SA position, going from stable Q-switch to chaos as the position is changed.

The laser output is recorded with a fast photodiode with a rise time of 100 ps, connected to a digital storage oscilloscope (PicoScope 6403B: 350 MHz bandwidth, 5 GS/s sampling rate, and 1 GS memory). We recorded the laser intensity over time while adjusting the SA position, resulting in 1,719 data sets, each containing between 6,000 and 50,800 pulses. For each data set, we extracted two time series, $s(n)$, one corresponding to the maximum intensity of each pulse and another with time between successive pulses, yielding a total of 3,438 time series.

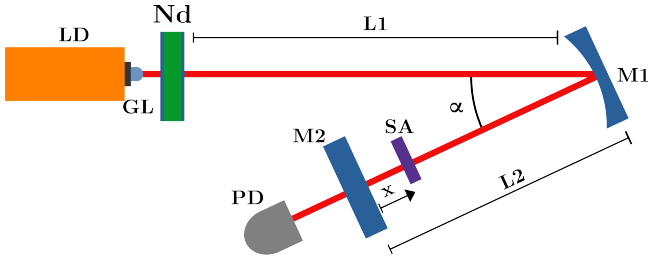


FIG. 1. Experimental setup of the Q-switched Nd:VO₄ laser. LD: pump laser diode. GL: GRIN lens. Nd: Nd:VO₄ crystal slab. L1 and L2: lengths of the first and second cavity arms (12 cm and 6 cm, respectively). α : angle between the cavity arms ($\approx 19^\circ$). M1: HR concave mirror with a radius of curvature of 10 cm. SA: Cr:YAG saturable absorber with 90% unbleached transmission. M2: plane output coupler with a reflectivity of 99%. x : distance between M2 and SA. PD: fast photodiode.

Attractor reconstruction and classification.— The embedding theorem [14, 15] states that an attractor's properties can be reconstructed from the time series of any system variable. In our case, we apply these techniques to the amplitude and time difference series. For each variable, we construct vectors in a d -dimensional space using $s(n)$ and its time delays, $s(n + T)$, as follows:

$$y(n) = [s(n), s(n + T), s(n + 2T), \dots, s(n + (d - 1)T)]. \quad (1)$$

By selecting the appropriate time delay and embedding dimension, d_E , the vector $y(n)$ reconstructs the phase space. This means that all motion invariants observed in the reconstructed time-delay space match those in the original space. Therefore, we can work in the reconstructed phase space and learn about the system as much as if we were working directly with the true space.

We define the time delay of the phase space, T , as the first minimum of the mutual information [16]. This criterion implies that the values of $s(n)$ and $s(n + T)$ are sufficiently independent to be used as coordinates in $y(n)$, while still maintaining some level of correlation. To determine the embedding dimension, we use the false nearest neighbors (FNN) method [17]. In this method, the proportion of false nearest neighbors (PFNN) is calculated as a function of the dimension, and d_E is defined as the dimension at which the PFNN approaches zero. Using these tools, the underlying attractor of a time series can be reconstructed, and its dynamics classified by computing the Lyapunov exponents, $\{\lambda_1, \lambda_2, \dots, \lambda_{d_E}\}$, and the fractal dimension.

The signature of a chaotic attractor is the presence of at least, one positive Lyapunov exponent [18]. The maximum exponent, λ_{max} , quantifies the degree of sensitivity to initial conditions. A negative sum of the Lyapunov ex-

ponents, $\sum_{i=1}^{d_E} \lambda_i$, indicates a dissipative system. Strange nonchaotic attractors require the computation of both the Lyapunov exponents and the fractal dimension. If both the sum of the Lyapunov exponents and λ_{max} are negative, the attractor is classified as nonchaotic. Furthermore, if the attractor has a non-integer fractal dimension, its dynamic is classified as strange nonchaotic.

We calculated the average mutual information, the proportion of FNN, and the Lyapunov exponents for each time series using the open source algorithms provided by Time Series Analysis (TISEAN) package [19]. For 10% of the analyzed time series, the mutual information could not be calculated, and T was set to 1. Figure 2a presents an example of the computed average mutual information for a time series of differences between successive pulses. In this example, the first minimum of mutual information occurs at a time lag of 1, after which the value decreases as the time lag increases. This behavior reflects the typical pattern observed in all time series where mutual information can be computed. The embedding dimension is defined as the dimension where the PFNN first drops below 15% and continues to decrease. A total of 32% of the time series meet this criterion and have a well-defined d_E . The remaining 68% of the time series, for which d_E could not be determined, are considered unclassified. We attribute this to the challenges in calculating FNN due to the noise in the experimental data. Figure 2b shows an example of the PFNN calculated as a function of dimension for the same example time series. In this case, d_E is equal to 3. This behavior also represents the typical pattern of PFNN in all time series where the embedding dimension is determinate. Figure 2c shows the reconstructed attractor for the example time series, calculated using equation (1). The figure clearly shows that the trajectories in the phase space are confined to a bounded region and do not expand to fill the entire space. This observation, which holds true for all time series where a finite embedding dimension was determined, indicates the presence of an attractor.

For the 1,096 time series whose attractors were reconstructed, we calculated their respective Lyapunov spectra. All of these series have a negative sum of Lyapunov exponents, and 94% have $\lambda_{max} > 0$, meaning that the series were chaotic. The remaining 6% of the time series exhibited a $\lambda_{max} < 0$, indicating that they were nonchaotic. We computed the energy spectral density for each nonchaotic time series. The spectra of all these series exhibit a broad frequency range, indicating that the dynamics are not periodic and that the dynamical regimes are complex. In Figure 3 can be seen the energy spectral density for a time series of the difference between successive pulses with $\lambda_{max} < 0$.

We applied Higuchi's method to estimate the fractal dimension, d_f , for each time series with $\lambda_{max} < 0$ [20]. This method constructs subsets of the time series using intervals of size k and measures the length of each

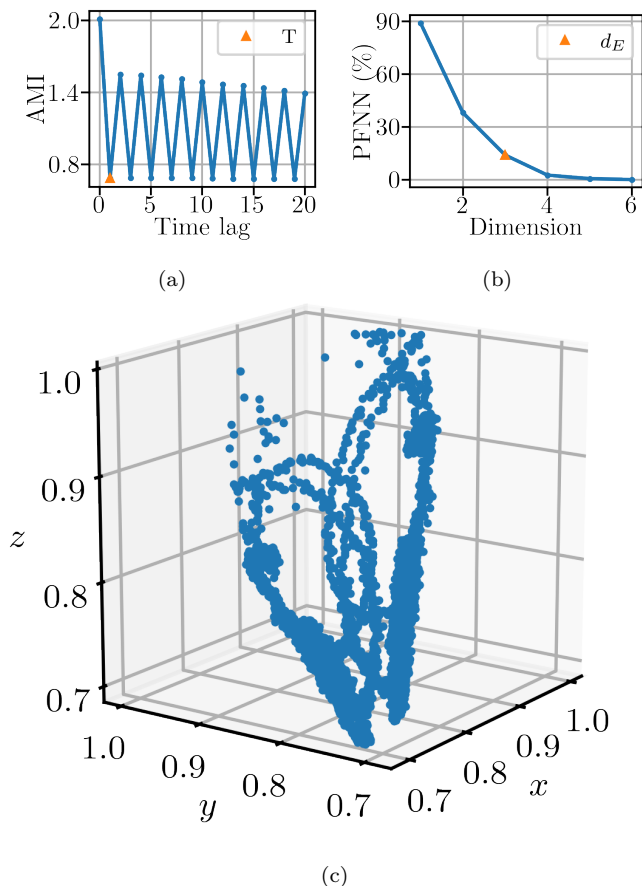


FIG. 2. Reconstruction of the attractor for a time series of difference between successive pulses. (a) Average mutual information (AMI) as a function of time lag. The blue dots mark the value of the average mutual information and the orange triangle the value of the first minimum, that in this case equals 1. (b) Proportion of false nearest neighbors. The blue dots are the value of the PFNN at each dimension. The orange triangle marks the embedding dimension, d_E , that in this case is equal to 3. (c) Reconstructed attractor. The axis x , y and z are $s(n)$, $s(n+1)$ and $s(n+2)$ components of equation (1) in arbitrary units.

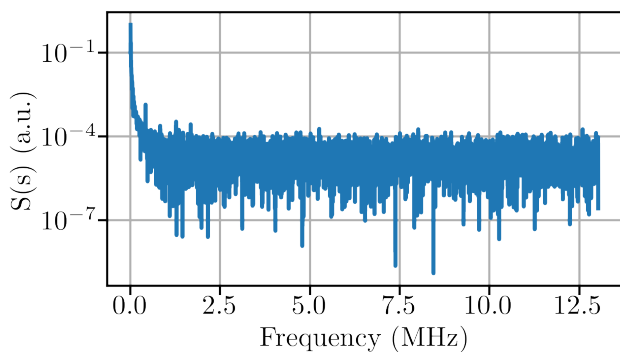


FIG. 3. Energy spectral density of a time series for a time series of difference between successive pulses.

subset, $L(k)$. If the relationship $L(k) \propto k^{-d_f}$ holds, the time series is fractal with dimension d_f . To verify this relationship, we plot $\ln L(k)$ against $\ln k$ on a doubly logarithmic scale. The data should align along a straight line with a slope of $-d_f$. In our case, we fit the straight line to the data using the least squares procedure. Higuchi's method recommends using a maximum value of k , k_{max} , that satisfies $k_{max} \leq N/10$, where N is the length of the time series. For all analyzed time series, we set $k_{max} = 100$, ensuring compliance with this condition. Figure 4 shows an example of this type of plot, where the estimated fractal dimension is $d_f = 2.70$. This example demonstrates a good fit, with a correlation coefficient $R = 1.0$. The fractal dimension could also be estimated for 147 of the total chaotic time series, with values ranging from 2.48 to 2.76. Similarly, among the nonchaotic time series, d_f could be reliably determined for 8 cases, with values ranging from 2.35 to 2.70. Therefore, we confirm that the underlying attractors of these 8 time series are strange nonchaotic, representing 0.2% of the total measured time series. The time series for which the fractal dimension could not be determined did not exhibit a well-defined $L(k) \propto k^{-d_f}$ relationship, likely due to the limitations of Higuchi's method when dealing with noisy data. As a result, their fractal dimension could not be estimated, and we cannot determine their dynamics are strange. However, given the nature of these series and their high complexity, their dynamics are not periodic. Table I presents a summary of the time series classifications.

To further characterize the reconstructed attractors with $\lambda_{max} < 0$, we calculated Kolmogorov complexity of each time series. Kolmogorov complexity (or Kolmogorov-Chaitin complexity) is a fundamental concept in algorithmic information theory that measures the computational resources needed to specify a binary sequence. The Kolmogorov complexity, K_c , of a string x , or any object represented as a binary string, is the length of the shortest possible program (in a fixed programming

TABLE I. Summary of the analyzed time series. The first column indicates the type of time series attractor. Where unclassified are time series for which d_E could not be determined. The second column shows the number of time series, M , for each attractor type. The third column lists the different values of time delay, T , the fourth column the different values of embedding dimension, d_E , and the fifth column shows the range of d_f values.

Attractor	M	T	d_E	d_f
unclassified	2342	—	—	—
chaotic	1029	1, ..., 17	3, ..., 6	2.48, ..., 2.76 ^a
nonchaotic	59	1	3, ..., 5	—
strange nonchaotic	8	1	4, 5	2.35, ..., 2.70

^a The fractal dimension was determined for 147 out of 1029 chaotic time series.

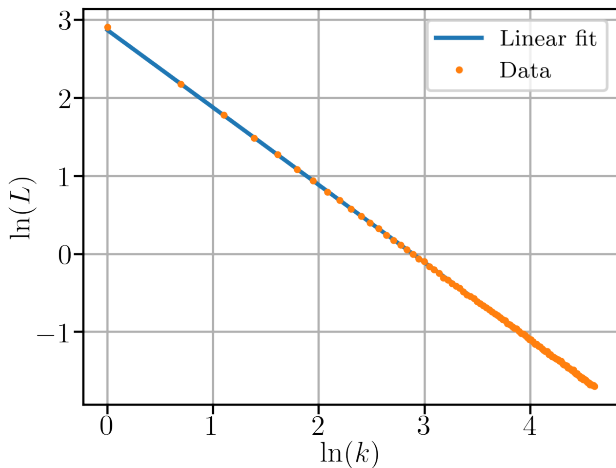


FIG. 4. Logarithm of the curve length $L(k)$ calculated using Higuchi's method for a time series of the difference between successive pulses. The straight line represents the linear fit, and its slope is the negative of the estimated fractal dimension. In this case d_f is 2.70.

language) that can produce x when run on a universal Turing machine. Unfortunately, K_c is uncomputable, so we use an approximation to estimate its value. K_c is related to the incompressibility of the string and provides a measure of unpredictability and complexity in an information sense. Each time series was binarized using its median value, and complexity was computed using the Mihailovic variant [21] of the Lempel-Ziv algorithm [22]. K_c is normalized to a scale where 0 corresponds to a perfectly predictable binarized time series (e.g., a periodic signal), and 1 represents a fully unpredictable (random) sequence. Intermediate values indicate complex nonperiodic dynamics. We find that the eight time series with all negative Lyapunov exponents and measured fractal dimensions exhibit K_c values ranging from 0.1 to 0.4. This intermediate range implies the time series is neither periodic nor random, but exhibits deterministic complexity which is a hallmark of SNAs.

Conclusions.— In summary, we have presented experimental evidence of the existence of a strange nonchaotic attractor in a passively Q-switched Nd:YVO₄ laser.

We measured the laser output intensity for several positions of the Cr:YAG and, for each data set, generated time series of maximum pulse intensity and inter-pulse intervals, resulting in a total of 3,438 time series. To analyze these time series, we reconstructed the underlying attractors by determining an optimal time delay and embedding dimension using mutual information and false nearest neighbors methods. We successfully reconstructed attractors for 32% of the time series. For these attractors, we calculated the Lyapunov exponents and found that 30% of the total time series exhibited a negative sum of Lyapunov exponents and a positive maxi-

mum exponent, indicating chaotic behavior. In contrast, the remaining reconstructed attractors, representing 2% of the total time series, exhibited both a negative sum of Lyapunov exponents and a negative maximum exponent, confirming their nonchaotic nature. Since these time series are non-periodic, we computed their fractal dimension using Higuchi's method. We obtained a well-defined fractal dimension for 12% of the time series with $\lambda_{max} < 0$.

The observed Kolmogorov complexity ($K_c = 0.1$ – 0.4) further supports the identification of a strange nonchaotic attractor (SNA). The intermediate K_c values reflect deterministic complexity consistent with fractal geometry, while the negative Lyapunov exponents exclude chaotic dynamics. This aligns with theoretical SNA signatures. Therefore, we conclude that these time series exhibit strange nonchaotic behavior. The strange nonchaotic time series represent only 0.2% of the total time series. To the best of our knowledge, this represents the first experimental observation of a strange nonchaotic attractor in an optical system.

Acknowledgments.— This work received support from the grants PUE 229- 2018-0100018CO and PIP 2022-00484CO CONICET (Argentina).

* jbourdieu@citedef.gob.ar

- [1] D. Ruelle and F. Takens, Les rencontres physiciens-mathématiciens de Strasbourg-RCP25 **12**, 1 (1971).
- [2] C. Grebogi, E. Ott, S. Pelikan, and J. Yorke, Physica D: Nonlinear Phenomena **13**, 261 (1984).
- [3] W. L. Ditto, M. L. Spano, H. T. Savage, S. N. Rauseo, J. Heagy, and E. Ott, Physical Review Letters **65**, 533 (1990).
- [4] T. Zhou, F. Moss, and A. Bulsara, Physical Review A **45**, 5394 (1992).
- [5] T. Yang and K. Bilimgut, Physics Letters A **236**, 494 (1997).
- [6] P. Durairaj, S. Kanagaraj, T. Kathamuthu, and K. Rajagopal, International Journal of Bifurcation and Chaos **32**, 2230022 (2022).
- [7] G. Ruiz and P. Parmananda, Physics Letters A **367**, 478 (2007).
- [8] C. Bracikowski and R. Roy, Chaos: An Interdisciplinary Journal of Nonlinear Science **1**, 49 (1991).
- [9] D. Pieroux and P. Mandel, Opt. Lett. **27**, 1528 (2002).
- [10] H. Haken, Physics Letters A **53**, 77 (1975).
- [11] J. Tang, Z. Bai, D. Zhang, Y. Qi, J. Ding, Y. Wang, and Z. Lu, Photonics **8**, <https://doi.org/10.3390/photonics8040093> (2021).
- [12] D. Dignowity and R. Ram  rez, Journal of Physics: Conference Series **23**, 149 (2005).
- [13] M. Kovalsky and A. Hnilo, Opt. Lett. **35**, 3498 (2010).
- [14] F. Takens, in *Dynamical Systems and Turbulence, Warwick 1980*, edited by D. Rand and L.-S. Young (Springer Berlin Heidelberg, Berlin, Heidelberg, 1981) pp. 366–381.
- [15] R. Ma  e, *Dynamical Systems and turbulence* (Springer - Verlag, Berlin, 1981).

- [16] A. Fraser and H. L. Swinney, Phys. Rev. A **33**, 1134 (1986).
- [17] M. B. Kennel, R. Brown, and H. D. I. Abarbanel, Phys. Rev. A **45**, 3403 (1992).
- [18] H. Abarbanel, *Analysis of observed chaotic data* (Springer - Verlag, Berlin, 1996).
- [19] R. Hegger, H. Kantz, and T. Schreiber, Chaos: An Interdisciplinary Journal of Nonlinear Science **9**, 413 (1999).
- [20] T. Higuchi, Physica D: Nonlinear Phenomena **31**, 277 (1998).
- [21] D. T. Mihailovic, G. Mimic, E. Nikolic-Djoric, and I. Arsenic, Open Physics **13**, doi:10.1515/phys-2015-0001 (2015).
- [22] A. Lempel and J. Ziv, IEEE Transactions on Information Theory **22**, 75 (1976).